International Journal of Sustainable and Green Energy
2019; 8(4): 65-80
http://www.sciencepublishinggroup.com/j/ijsge
doi: 10.11648/j.ijrse.20190804.11
ISSN: 2575-2189 (Print); ISSN: 2575-1549 (Online)

Wind Turbulence Intensity Characteristics at 10m Above Ground Along the Cotonou Coast, Benin

Hagninou Elagnon Venance Donnou*, Aristide Barthélémy Akpo, Julien Djossou, Basile Bruno Kounouhewa

Laboratory of Radiation Physics, University of Abomey-Calavi, Cotonou, Benin

Email address:

donhelv@yahoo.fr (H. E. V. Donnou), akpoarist@yahoo.fr (A. B. Akpo), jdjossou32@yahoo.fr (J. Djossou), kbbasile@gmail.com (B. B. Kounouhewa)

*Corresponding author

To cite this article:

Hagninou Elagnon Venance Donnou, Aristide Barthélémy Akpo, Julien Djossou, Basile Bruno Kounouhewa. Wind Turbulence Intensity Characteristics at 10m Above Ground Along the Cotonou Coast, Benin. *International Journal of Sustainable and Green Energy.* Vol. 8, No. 4, 2019, pp. 65-80. doi: 10.11648/j.ijrse.20190804.11

Received: October 14, 2019; **Accepted**: November 12, 2019; **Published**: November 25, 2019

Abstract: The characteristics of the wind turbulence intensity that are essential to know before installing a wind turbine at a site were investigated along the coast of Cotonou in Benin. The average speed, direction, roughness length, friction velocity, turbulence intensity and relationship between the roughness and wind turbulence intensity were evaluated as well. Using the estimators derived from a simple isotropic Gaussian model of turbulent wind fluctuations, we proposed modified models for estimating the turbulence intensity of wind components. Wind speed and direction data recorded at 10 m above ground level from 2011 to 2014 during the first Compact of the Millennium Challenge Account (MCA) in Benin were utilized. The results obtained indicated that the annual average roughness length is evaluated at 1.25×10^{-4} m, and the annual mean friction velocity is equal to 0.41 $m.s^{-1}$. Peak values of the turbulence intensity vary from 0.3 to 0.6 except during the months of January, April, July, August and September. The high values obtained could jeopardize the production of wind energy during these months. The correlation between the turbulence intensity and roughness length ranging from 0.75 in January to 0.94 in August revealed that these two parameters are linked by an increasing linear function. Finally, modified formulations of the longitudinal and transversal wind turbulence intensity developed from the van den Hurk and de Bruin model and based on the best-fitting approach were proposed. The error estimators (MAE; RMSE) computed to validate these modified models vary respectively from (0.0099; 0.0141) to (0.0614; 0.0890).

Keywords: Turbulence Intensity, Surface Roughness Length, Friction Velocity, Modified Estimators

1. Introduction

Electricity generation from wind turbines has gained momentum over the past two decades [1]. The worldwide cumulative installed wind capacity increased from 23,900 MW in 2001 to 539,581 MW in 2017 with a growth rate of about 2000%, which deserves to be valorized in underdeveloped countries [2, 3] particularly in Benin. Moreover, this technology can contribute greatly to long-term economic growth of these countries, ensuring energy independence and boosting their local economy [4]. Wind power extraction involves using rotor blades which are the most important part of the aerodynamic device, owing to their profiles. Recently, Rafiee *et al.* (2016) and Boumrar (2016) [5, 6] have shown that during their operation, and due to harsh and varied environmental conditions, those blades are exposed to complex cyclic loadings which induce static or even dynamic stresses. Thus, the decline in energy production, component failures inside and outside wind turbines, including motors, gears, and also cracks on wind turbine blades have occurred in the operation of wind turbines [7], reducing thus the performance of wind farms built offshore and onshore. As mentioned earlier, [1, 8-20] pointed out that wind turbulence effects at low frequencies have been the major cause of these problems. In addition, due to the sudden changes in wind direction and speed, these effects prompt blade fatigue which is the main source of

reduction in the lifetime of wind turbines [21-25]. To better understand the behavior of such a turbulent system, therefore, a correct modeling of these fluctuations is crucial for estimating the fatigue loads on wind turbine blades [26]. Longitudinal and transversal wind fluctuations which provide important information on the turbulence properties in the atmospheric boundary layer [27] are therefore essential inputs for turbulence intensity estimation models that are instrumental in the design and operation of wind turbines [28]. The choice of turbines and their precise location, then, entail a more accurate determination of wind turbulence conditions, taking into account local factors [29]. Considering the major investment in this sector, with the installation of many large wind farms and other projects under planning, the blade design optimization is vital in order to improve their performance [30]. Thus, specific investigations into the local wind characteristics at low-frequencies (which constitute an appropriate scale for wind energy production) [16, 31] must be made whatever the site before wind turbine installation, as recommended by [32, 33].

According to [31], West Africa is subject to significant wind fluctuations and seasonal changes due to the movement of trade winds (hot or humid air flow) and thermal winds. Likewise, Benin's coast, one with a considerable wind potential [34-36], is also exposed to this wind variability according to [37] and likely to reduce the life span of wind turbines. It is, therefore, imperative to conduct this study in this area of Benin where research work has focused on wind energy potential assessment only.

Our aim is to investigate the wind characteristics at 10 m above ground along the coast of Cotonou (Benin) ones, the knowledge of which is necessary before the installation of a wind turbine at a site. In this respect, the present article seeks to:

1. determine the wind direction and mean wind speed at low-frequency;
2. evaluate the roughness length, friction velocity and turbulence intensity;
3. establish the correlation between the roughness and turbulence intensity;
4. propose new estimators for the turbulence intensity of wind components.

2. Material and Methods

2.1. Material

2.1.1. Study Area Description

Benin is situated in the Gulf of Guinea (see Figure 1) between latitude 6°15' N and 12°30' N on the one hand and longitude 1°E and 3°40' E on the other. Its coastline is 125 km long and extends from Hillacondji in the West to Kraké in the East. This strip of land is located between latitude 6°15' N and 7°00' N.

Figure 1. *Benin coastal area, Gulf of Guinea.*

2.1.2. Data Collection

We used a series of wind parameter measurements (wind speed and direction) performed by the Millennium Challenge Account (MCA) compact I and the Beninese Institute for Fishery and Oceanographic Research (IRHOB in French). This measurement campaign spans the period from June 1st, 2011 to April 30th, 2013 and that from December 1st, 2013 to April 30th, 2014. The measurements were recorded every 10-minute, using a cup anemometer and weather vane installed at 10 m above ground level. Figure 2 shows the wind sensor position together with the data logger (receiving station), both of which are located at the seaside.

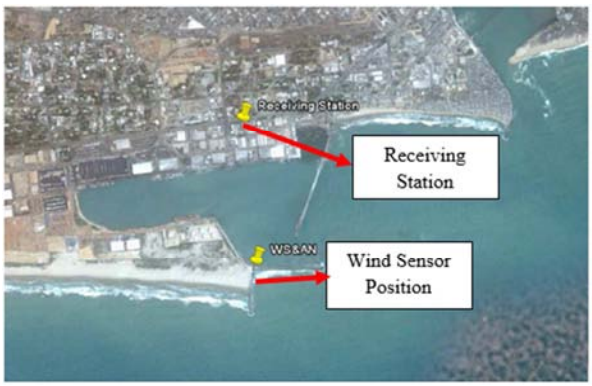

Figure 2. *Wind sensor and data logger (receiving station) position at the seaside [38].*

2.2. Theory

2.2.1. Friction Velocity

In the surface layer, the flow is governed by the Monin-Obukhov similarity theory. Several methods have been used based on this theory to evaluate the statistical turbulence variables (friction velocity, surface roughness length, Obukhov length, etc.) [39-44]. We determined the surface friction velocity u_* using the momentum flows $\overline{u'v'}$ (covariance of vertical and longitudinal wind component) and $\overline{v'w'}$ (covariance of vertical and transversal wind component) along with the Monin-Obukhov theory:

$$u_* = \left(\overline{u'v'}^2 + \overline{v'w'}^2\right)^{1/4} = \left[\left(\mathrm{cov}(u,w)\right)^2 + \left(\mathrm{cov}(v,w)\right)^2\right]^{1/4} \quad (1)$$

where u is the longitudinal wind component and v the transversal wind component.

We used the Cauchy-Schwarz inequality theory $\left[\mathrm{cov}(x,y)\right]^2 \le \sigma^2(x)\sigma^2(y)$ (where x and y are variables) to calculate the covariance. The wind vertical component in Equation (1) is not directly measured by our cup anemometer. Thus, we calculated its standard deviation (σ_w) from the standard deviation of the horizontal wind speed (σ_U), using given by [45]:

$$\sigma_w = 0.45\sigma_U \quad (2)$$

The cup anemometer provides the horizontal wind speed data and the weather vane provides the wind direction data. As, u and v are not directly measured, we used Equation (3) given by [46]:

$$\begin{cases} u = U\sin\left((\theta+180)*\left(\pi/180\right)\right) \\ v = U\cos\left((\theta+180)*\left(\pi/180\right)\right) \end{cases} \quad (3)$$

where U is the average horizontal wind and θ the Wind direction (in degrees).

The variances of the wind components (longitudinal (σ_u^2), transversal (σ_v^2) and horizontal (σ_U^2)) were respectively obtained using Equations (4) and (6) [47]:

$$\sigma_u^2 = \frac{1}{n-1}\sum_{i=1}^{n}\left(\bar{u} - u_i\right)^2 \quad (4)$$

$$\sigma_v^2 = \frac{1}{n-1}\sum_{i=1}^{n}\left(\bar{v} - v_i\right)^2 \quad (5)$$

$$\sigma_U^2 = \frac{1}{n-1}\sum_{i=1}^{n}\left(U - U_i\right)^2 \quad (6)$$

where n is the observation number, $\bar{u}$ the longitudinal wind mean, and $\bar{v}$ the transversal wind mean.

2.2.2. Surface Roughness Length

In practice, it is difficult to determine this parameter experimentally with precision. But, we approximated it using the model of [48-50]:

$$z_0 = \frac{\alpha_c u_*^{\,2}}{g} \quad (7)$$

where g is the gravity, α_c varies from about 0.011 on sea surface to 0.018 in coastal areas [51, 52]. α_c = 0.018 was used in this study.

2.2.3. Wind Turbulence Intensity

Here, we calculated the turbulence intensity (I) which is the ratio between the wind speed standard deviation and the horizontal wind module, every 10 minutes as was done by [31, 53-55], using Equation (8):

$$I = \frac{\sigma_U}{U} \quad (8)$$

The longitudinal and transversal wind turbulence intensity is, thus, respectively given by [56]:

$$I_u = \frac{\sigma_u}{U} \quad (9)$$

$$I_v = \frac{\sigma_v}{U} \quad (10)$$

2.2.4. Model for Estimating I_u and I_v

For estimating the fatigue loads on wind turbine blades, the turbulence intensity estimation models are input parameters. Several methods that can be used to estimate σ_u and σ_v from wind speed and direction statistics have been reported by [45, 27]. These models are based on a simple isotropic Gaussian model of turbulent wind fluctuations. One of the best estimators for the fluctuations of wind components according to these authors is the model of [57]. It is expressed by:

$$\sigma_u^2 = \sigma_v^2 = \frac{1}{2}\left\{\sigma_U^2 - U^2\left[\exp\left(-\sigma_\theta^2\right) - 1\right]\right\} \quad (11)$$

where σ_θ is the standard deviation of wind direction.

Luhar (2010) [27] contends that this model clearly takes σ_U into account and, therefore, its performance is much

better. However, he noticed some inconsistencies, particularly the hypothesis about the equality between σ_u and σ_v in the van den Hurk and de Bruin model. He then proposed a more consistent set of relations for σ_u^2 and σ_v^2 (Equations (12) and (13)) based on the approach of [58], thereby assuming that U and θ are statistically independent and that θ is normally distributed:

$$\sigma_u^2 = u^2\left\{\cosh\left(\sigma_\theta^2\right)\left[1+\left(\frac{\sigma_U}{u}\right)^2\exp\left(-\sigma_\theta^2\right)\right]-1\right\} \quad (12)$$

$$\sigma_v^2 = u^2\sinh\left(\sigma_\theta^2\right)\left[1+\left(\frac{\sigma_U}{u}\right)^2\exp\left(-\sigma_\theta^2\right)\right] \quad (13)$$

These models (Equations (11) to (13)) were used to estimate the components of wind turbulence intensity based on Equations (9) and (10). Next, these estimations were evaluated comparing them to our site data. From their respective performance, modified formulations were proposed according to an optimal approach. The method adopted to reach this objective is presented in section 3.2.5.

2.2.5. Correlation Test

We calculated the error estimators between the turbulence intensity models and data using the Root Mean Square Error (RMSE) and the Mean Absolute Error (MAE) that measure the average magnitude of errors made by the forecast. We also evaluated a quantitative correlation between the turbulence intensity and the roughness using the Pearson correlation test. These estimators are the indicators used the most and calculated with the formulas below [59-61]:

$$RMSE = \sqrt{\frac{1}{n}\sum_{i=1}^{n}\left(p_i - f_i\right)^2} \quad (14)$$

$$MAE = \frac{1}{n}\sum_{i=1}^{n}\left|p_i - f_i\right| \quad (15)$$

$$R = \frac{\sum_{i=1}^{n}\left(p_i-\overline{p}\right)\left(f_i-\overline{f}\right)}{\sqrt{\sum_{i=1}^{n}\left(p_i-\overline{p}\right)^2\sum_{i=1}^{n}\left(f_i-\overline{f}\right)^2}} \quad (16)$$

p_i : Observations, $\overline{p}$: Average of observations, f_i : Estimations, $\overline{f}$: Average of estimations, n: Total observation number.

The smaller the error estimator value is and tends to zero, the better the model is (Akpinar and Akpinar 2007). As to R, it varies from 0 to 1. If $R=0$, there is no linear correlation between the estimations and observations. If $R=1$, the predictions have been perfectly correlated with the observations. When R is near 1, the correlation is very good.

3. Results and Discussion

3.1. Average Flow Characteristics

3.1.1. Monthly Average Distribution of the Horizontal Wind

The boxplot of the monthly average distribution of the horizontal wind speed is presented in Figure 3.

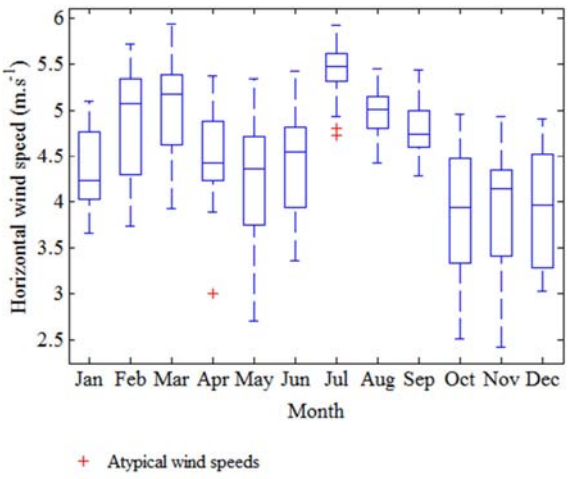

Figure 3. *Monthly boxplot of the horizontal wind speed (2011-2014).*

Figure 3 indicates that the average wind distribution is not homogeneous during the year, but has two peaks. We recorded the first peak in March with a monthly average speed of 5.02 m.s^{-1} and the second peak was observed in July with a monthly average speed of about 5.46 m.s^{-1}. The first peak would be due to the strong air mass convection observed during this hottest month of the year (Ogbonmwan *et al.* 2016). As to the second peak, it is due to the presence of the West African monsoon during this period of the year which pushes the intertropical front (ITF) towards the Sahel in the North [62] (Ogbonmwan et al. 2016). The least windy months are October, November and December, with the monthly average speeds between 3.88 and 3.94 m.s^{-1}. The gradual arrival of the north-east Asian trade winds (Harmattan) leading to a southward movement of the intertropical front (ITF) during this period of the year explains the low speeds observed. The lowest daily average speed during the year was observed in November and evaluated at 2.41 m.s^{-1}, but the highest speed was recorded in July with an average of about 5.92 m.s^{-1}. We also noted that the atypical wind speeds were estimated at 3 m.s^{-1} in April, and vary between 4.93 and 4.98 m.s^{-1} in July. These different results obtained reveal that the great wind variability at our site could cause energy production problems at the blade level. As it was stated above (see Equation (8)), fluctuations vary according to wind speed and turbulence intensity.

3.1.2. Daily Average Distribution of the Horizontal Wind

Figure 4 presents the monthly daily distribution of the horizontal wind speed.

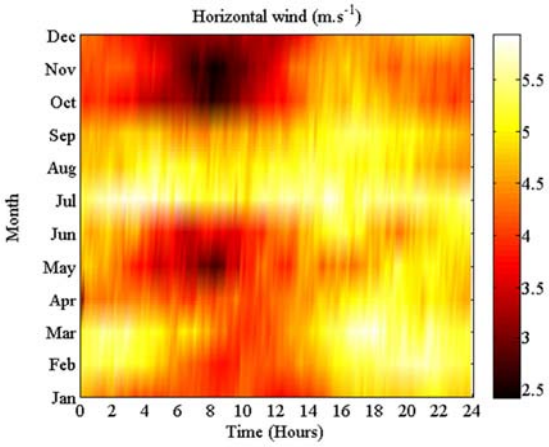

Figure 4. *Monthly daily distribution of the horizontal wind speed (2011-2014).*

Figure 4 shows that from January to June the horizontal wind is generally strong after 15:00 and evaluated on average at 5.3 m.s^{-1}. Apart from the months of February and March, the peaks evaluated at 5 m.s^{-1} were observed between 00:00 and 06:00. During the other periods of the day (between 06:00 and 14:00), winds are generally light with an average of 3.3 m.s^{-1}. From July to September, the diurnal and nocturnal wind cycles are characterized with rather high winds compared to other periods of the year. Between July and August, the horizontal wind varies from 4.8 m.s^{-1} to 5.92 m.s^{-1} in July and from 4.42m.s^{-1} to 5.41 m.s^{-1} in August. In September the same observations were made with winds ranging from 4.28 m.s^{-1} to 5.43 m.s^{-1}. Next, we noticed that, between October and December, the trend is reversed with winds having low speeds from 04:00 to 11:00, and relatively high speeds, from 00:00 to 04:00 and from 11:00 to 23:50. The average wind speed fluctuates from 2.5 m.s^{-1} to 4.95 m.s^{-1} in October, 2.41 m.s^{-1} to 4.93 m.s^{-1} in November, and 3.02 m.s^{-1} to 4.91 m.s^{-1} in December.

3.1.3. Daily Average Distribution of the Longitudinal and Transversal Wind

Figures 5 and 6 highlight the monthly daily variations of the longitudinal and transversal wind components.

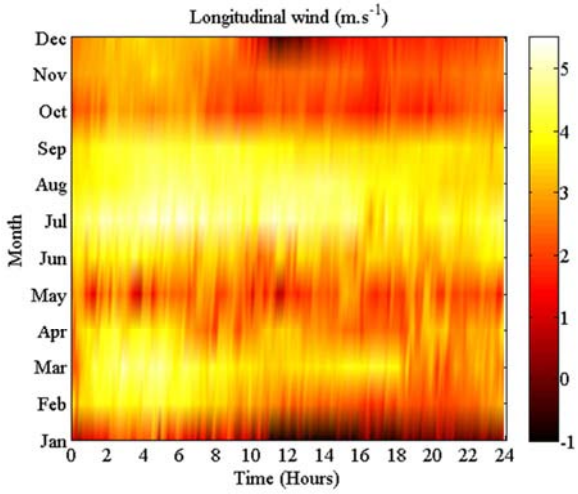

Figure 5. *Monthly daily distribution of the longitudinal wind (2011-2014).*

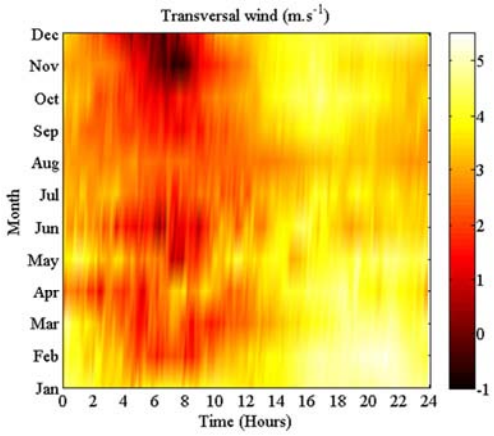

Figure 6. *Monthly daily distribution of the transversal wind (2011-2014).*

In Figure 5, we generally noted that the longitudinal wind component is low in January. But, from February to March, high longitudinal winds were recorded. These values vary from 01:00 to 10:00 in February and from 01:00 to 18:00 in March. High winds were also observed in April between 01:00 and 06:00, and they become relatively low during the rest of the day. In June, the longitudinal wind speeds increase again before reaching the maxima of the year observed between July and August and evaluated at 5.34 m.s^{-1}. From September, the longitudinal wind amplitude starts decreasing again until December. Negative values are also recorded for the longitudinal wind in December and January due to the predominance of the north-east trade winds during this period of the year. In Figure 6, the variations of the meridional wind are not similar to those of the longitudinal wind. Indeed, the peak of the year is observed between January and February with a speed estimated at 5.32 m.s^{-1} in February. From 01:00 to 13:00, the meridional wind reaches its lowest values whatever the period of the year, except January to March and in May between 00:00 to 02:00. From 13:00 to 23:50, the values were relatively higher. Between 06:00 and 08:00 from November to December the negative amplitudes of the meridional wind are noticed and due to the presence of northwesterly winds during this period.

3.1.4. Annual Daily Distribution of the Horizontal, Longitudinal and Transversal Wind

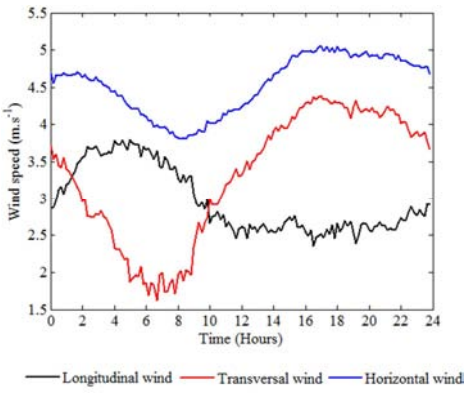

Figure 7. *Annual daily distribution of the longitudinal, transversal and horizontal wind (2011-2014).*

We present here the annual daily wind distribution of the longitudinal, transversal and horizontal wind components (see Figure 7).

We noted that the annual average amplitude of the transversal wind increases during the day between 07:00 and 17:00 with a speed varying from 1.62 $m.s^{-1}$ to 4.38 $m.s^{-1}$. After 17:00 the amplitude decreases until 07:00 and reaches its lowest daily speed evaluated at 1.62 $m.s^{-1}$. The opposite phenomenon was observed with the annual mean of the longitudinal wind. The peak of this component is reached early in the morning around 05:00 with a speed of 3.79 $m.s^{-1}$. During the rest of the time, the amplitude of the zonal wind decreases before increasing again after 22:00. From 10:00 to 01:00, the transversal wind dominates the longitudinal wind. This trend is reversed from 01:00 to 10:00. As to the annual average speed of the horizontal component, it has two peaks. The first peak is less noticeable around 01:40 with an average speed of 4.73 $m.s^{-1}$ and the second one is recorded around 17:00 and corresponds to 5.05 $m.s^{-1}$. During the day from 08:30 to 17:00 we noticed an increase in the horizontal wind speed from 3.8 $m.s^{-1}$ to 5.05 $m.s^{-1}$ and, after 17:00, a progressive decrease down to 3.8 $m.s^{-1}$.

3.1.5. Wind Rose

The wind rose obtained at the Cotonou site is illustrated in Figure 8.

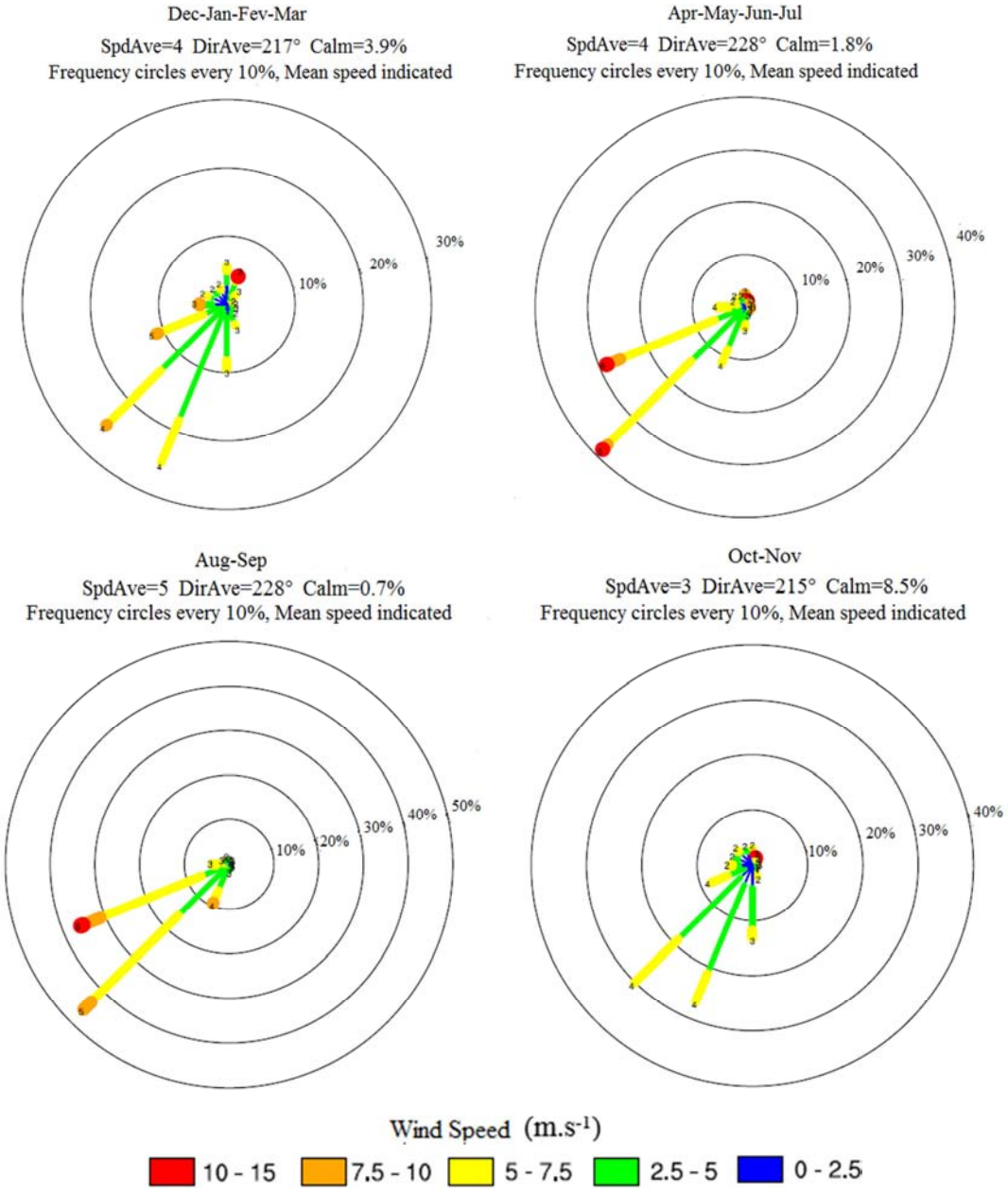

Figure 8. *Wind rose according the seasons of the year at 10 m above ground (2011-2014).*

Figure 8 shows the wind rose according to the four seasons observed during the year at the site of Cotonou:

long dry season (December to March), long rainy season (April to July), short dry season (August to September) and short rainy season (October to November). It can then be noticed that the vast majority of winds come from the south. The southwest (SW) and south-southwest (SSW) directions are the most dominant ones whatever the seasons. Their frequency of occurrence varies from 25 to 45% with instantaneous wind speeds in the order of 5 to 15 $m.s^{-1}$. This predominance is caused by the frequent sea breezes on the coast of Benin and the West African monsoon prevailing in the study area at the end of May and extending until September [63]. Winds coming from the North (N) with a speed of 5 to 7.5 $m.s^{-1}$ and those from the north-east (NE) with a speed between 10 and 15 $m.s^{-1}$ were mostly observed in the long dry season– with a low frequency of the order of 5%. Some southeast (SE) winds occur with less than 5% as well as some westerly (W) winds noticed during the long dry and rainy seasons, with speeds varying from 5 to 10 $m.s^{-1}$. The presence of some westerly (W) and northwesterly (NW) winds was also noted in the study area. During the year except the long dry season there are practically no northerly winds. The arrival of Harmattan in our study area at the end of December until mid-January explains the rare occurrence of the prevailing southerly winds (25%) in the long dry season.

3.2. Characteristics of the Turbulent Flow at Low-Frequency

3.2.1. Distribution of Horizontal Wind Fluctuations

Figure 9 shows the monthly daily wind fluctuations.

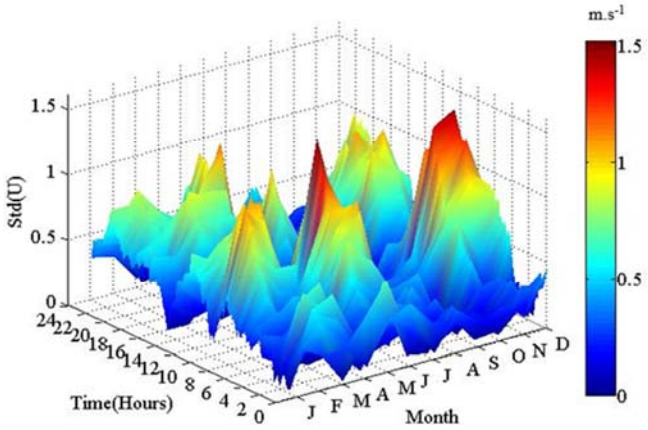

Figure 9. *Monthly daily fluctuations of the horizontal wind (2011-2014).*

In figure 9, the daily distribution of the horizontal wind fluctuations varies from 5×10^{-4} to 1.51 $m.s^{-1}$ whatever the period of year. The highest fluctuations of the horizontal wind were recorded between 08:00 and 14:00 during the months of February, March, May, June, October November and December. The peaks vary from 0.9 to 1.51 $m.s^{-1}$ and were obtained in December and May respectively. The low values of the fluctuations were recorded in January, April, July, August and September. As pointed out by [31], these values are, then, indicative and reveal the presence of significant wind fluctuations in West Africa, particularly in Benin according to [37]. Likewise, the monthly average of the standard deviation varies from 0.17 $m.s^{-1}$ in July to 0.55 $m.s^{-1}$ in November.

3.2.2. Characteristics of the Statistical Turbulence Variables

Based on Equations (1) to (7), the daily variations of the roughness length and the surface friction velocity at the site of Cotonou on a monthly scale have been respectively presented in Figures 10 and 11.

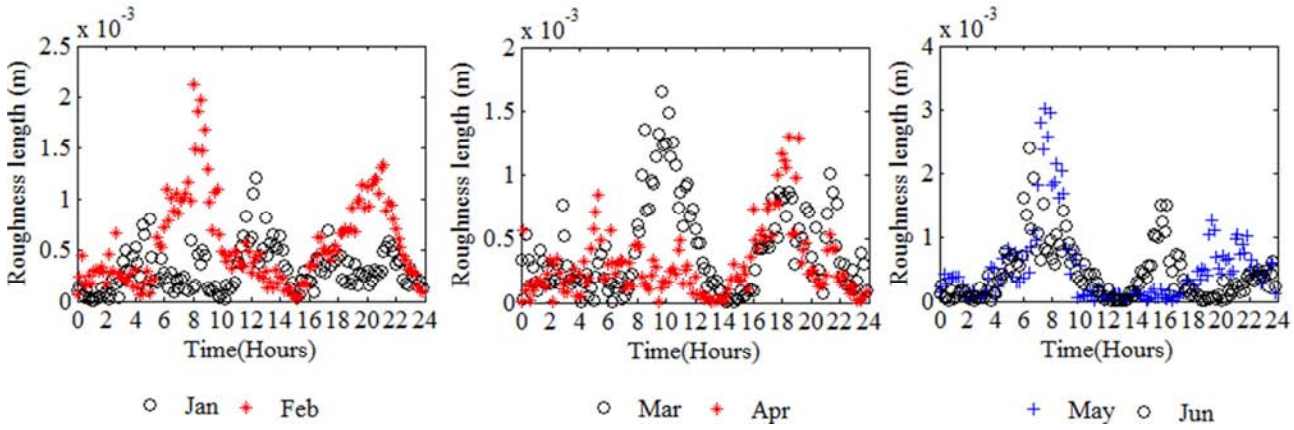

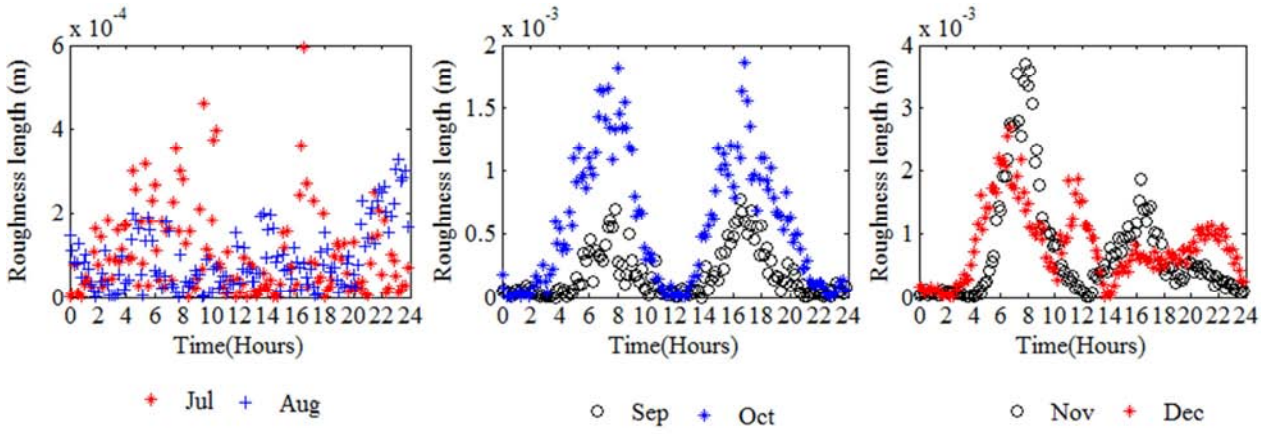

Figure 10. *Daily variations in the roughness length on a monthly scale (2011-2014).*

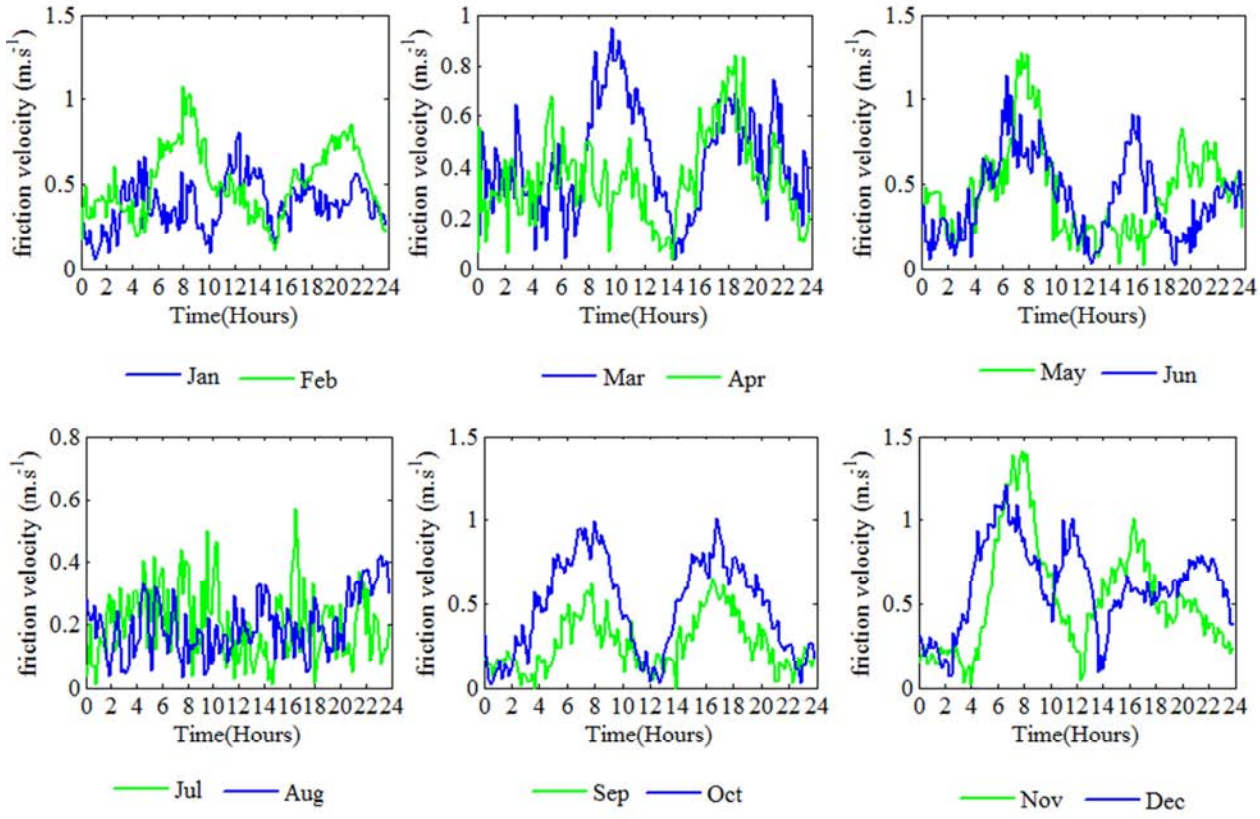

Figure 11. *Daily variations in the surface friction velocity on a monthly time scale (2011-2014).*

The surface roughness obtained during the year reached the values of 10^{-4} to 10^{-3} m. During the diurnal cycles the values were on average higher than those in the nocturnal cycle. The low roughness values were obtained from July to September with a peak of about 6×10^{-4} m recorded in July. In the other months, the roughness values are higher. The peaks observed in May, November and December vary from 3×10^{-3} m to 4×10^{-3} m. The annual average roughness length was estimated at 1.25×10^{-4} m. The low roughness values obtained at our site could be due to the wind sensor position which is located by the seaside (as shown in Figure 2). Moreover, the most frequent wind directions at the site come from the sea (south-southwest, southwest direction as illustrated in Figure 8). These results are close to those obtained by [49, 64], who worked on similar sites and proposed values of about 10^{-4} m. The variations in the friction velocity indicate that this parameter reached a peak of 1.45 $m.s^{-1}$ in November. The monthly average varies between 0.20 $m.s^{-1}$ in August and 0.61 $m.s^{-1}$ in December. The annual average was estimated at 0.41 $m.s^{-1}$. These different results are also close to those found by [65, 66] at coastal sites and estimated at 0.55 $m.s^{-1}$ and 0.43 $m.s^{-1}$ respectively.

3.2.3. Characteristics of the Wind Turbulence Intensity

The wind turbulence intensity was calculated and the different daily distributions are exemplified in Figure 12.

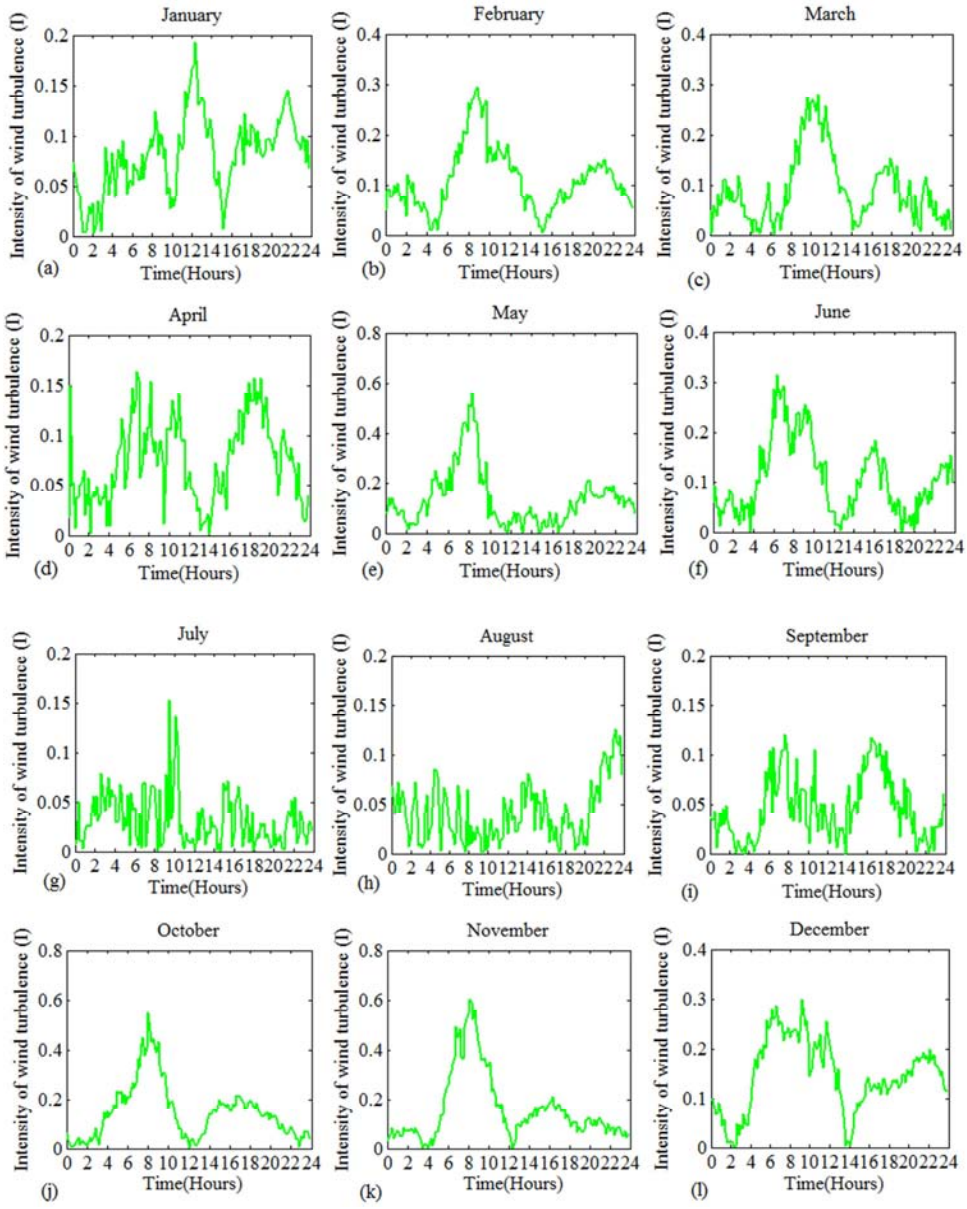

Figure 12. *(a-l) Daily distribution of the wind turbulence intensity from January to December (2011-2014).*

The wind turbulence intensity and the surface roughness have the same daily distribution which correlates with the friction velocity (see Figure 12). The highest values of the turbulence intensity were observed in May, October as well as November and evaluated at 0.6. The lowest values were obtained in January, April, July, August, and September with the peak value (0.19) recorded in January. During the other months (February, March, June, and December), the peak values obtained were evaluated at 0.3. Martin et al. [13] showed that the turbulence is high when the peak value exceeds 0.2. Moreover, experimentally, [7] concluded that the threshold value of the turbulence intensity to be used with respect to the optimal planning of wind turbine installation is 0.2. [8-11, 15, 16, 67, 68] asserted that high values of the turbulence intensity have a negative influence on wind turbine blades, especially their lifetime, and lead to a fall in energy production. In conducting wind tunnel experiments, [11] showed that when the wind turbulence intensity increases from 5% to 25%, the wind turbine performance decreases nearly from 23% to 42%. As to the work of [69], the authors believe that a site with higher turbulence intensity has a lower wind power potential and, thus, is less attractive for wind power application. Relying on their work, we can therefore conclude that February, March, May, June and October to December are unfavourable for an efficient use of this energy source. On the other hand, January, April, July, August and September are favourable for wind energy production. Before the installation of wind turbines at our study site, we then suggest taking into account the fatigue loads induced by high turbulence levels observed at the site in the design of wind turbine blades in order to optimize energy production and ensure a long lifetime of wind turbines.

3.2.4. Turbulence Intensity Estimation from the Roughness Length

Figure 13 shows the monthly correlation between the turbulence intensity and roughness. Different linear equations for estimating the turbulence intensity based on the roughness length were proposed. Pearson's correlation coefficient was determined in order to validate these equations.

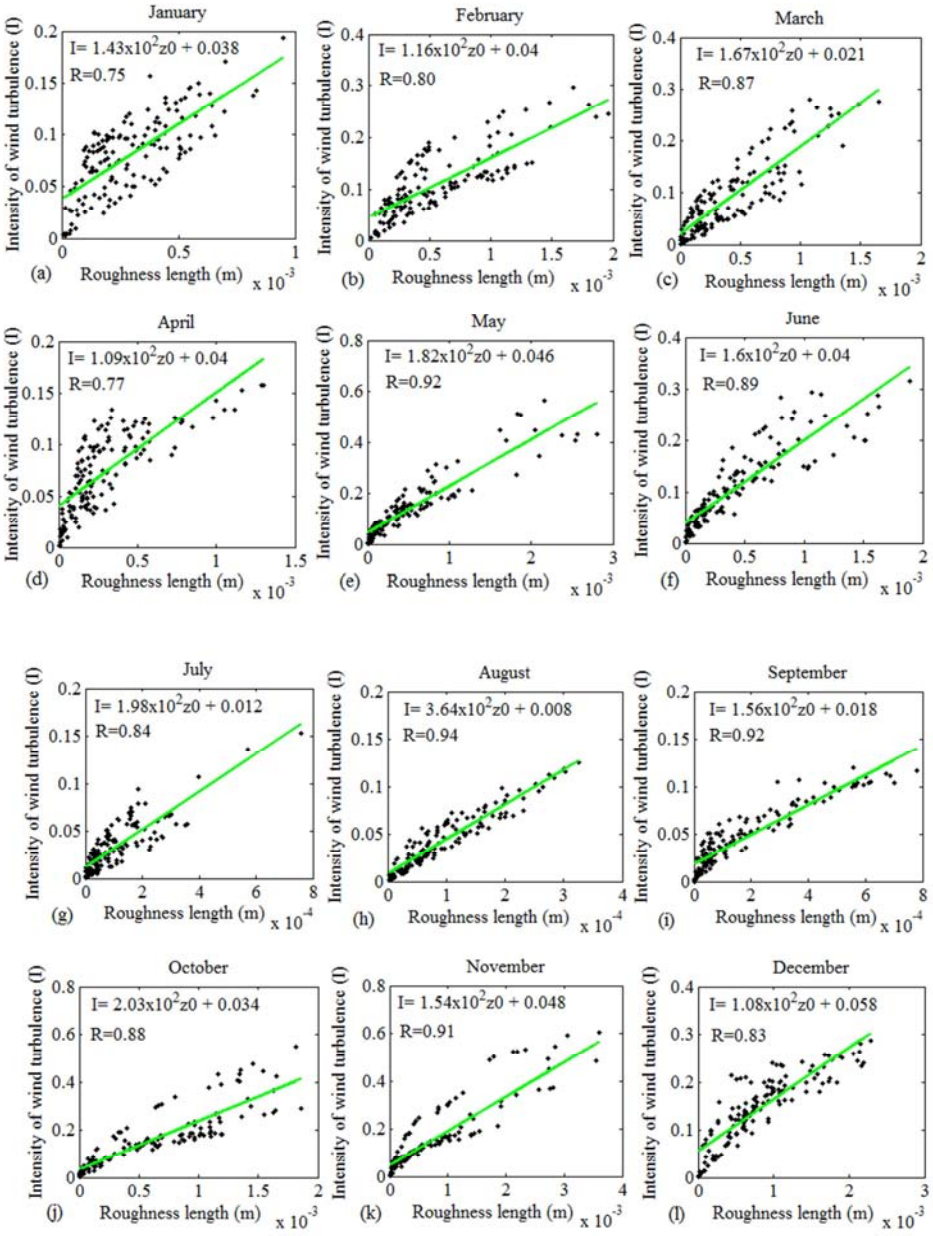

Figure 13. *(a-l) Linear adjustment between turbulence intensity and roughness length from January to December (2011-2014).*

Analysis of Figure 13 reveals that the turbulence intensity and roughness length generally display a pretty good correlation. Indeed, Pearson's correlation coefficient varies from 0.75 in January to 0.94 in August. During May, August, September, and November the correlation between the two parameters evaluated at (0.92; 0.94; 0.92; 0.91) respectively is good and better than that in other months. In February, March, June, July, October and December this correlation is moderately good. Pearson's correlation coefficient varies from 0.80 to 0.89. In January and April we noticed that the correlation is less good compared to the other months and between 0.75 and 0.77. These different values of Pearson's correlation coefficient allow us to validate the use of the different linear adjustments proposed to calculate the turbulence intensity based on the roughness at our site. In short, turbulence intensity is an increasing function of roughness. This observation is consistent with the findings obtained by [70-73].

3.2.5. Fitting of the Turbulence Intensity of Wind Components

In Figure 14, we compared the adjustment curves of the longitudinal and transversal wind turbulence intensity distribution obtained from van den Hurk and Bruin, Luhar models (Equations (9) to (13)) and from turbulence intensity data.

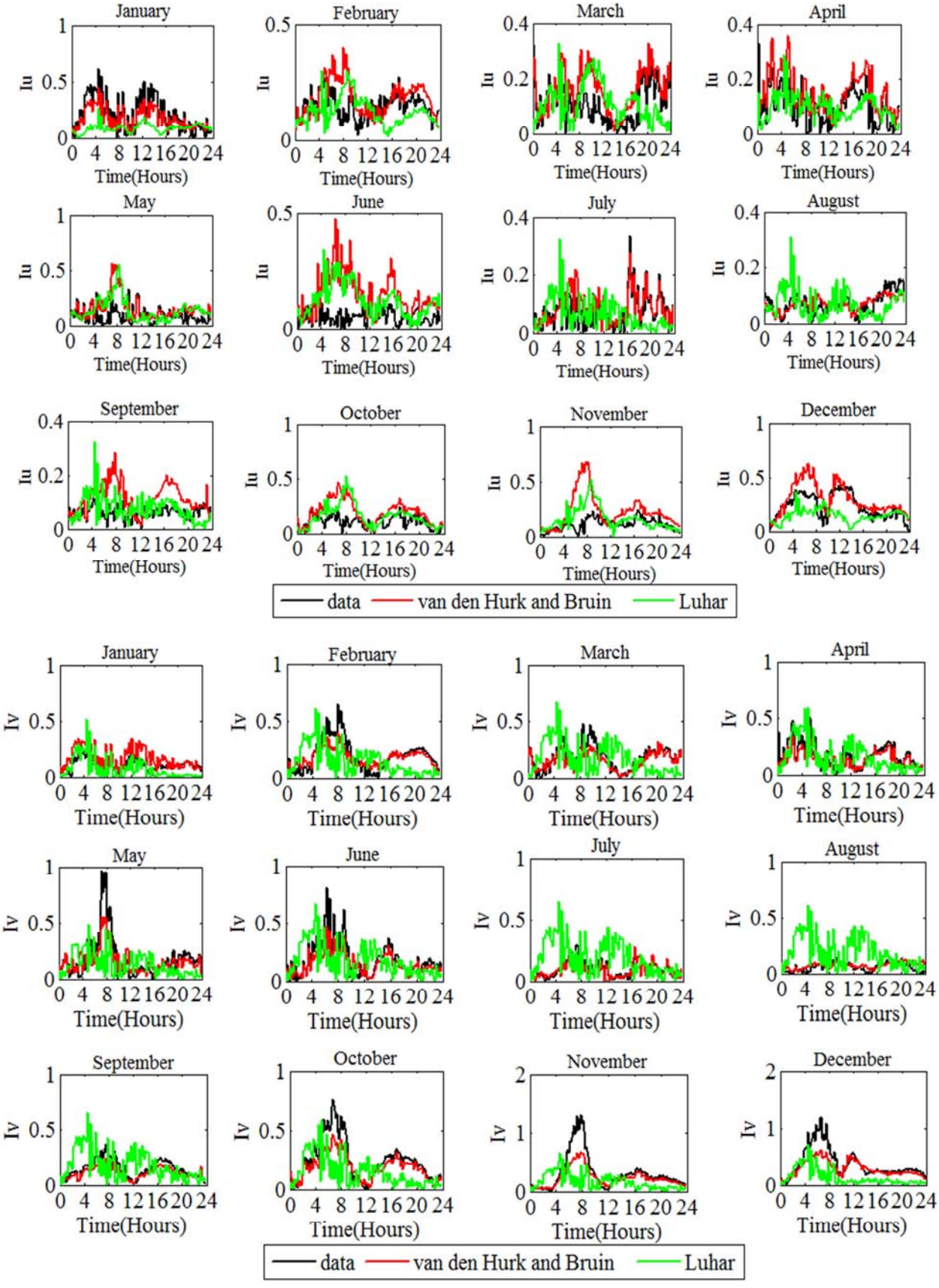

Figure 14. *Turbulence intensity model evaluation of the longitudinal and transversal wind component (I_u , I_v) (2011-2014).*

In Table 1 are presented the error estimators (MAE, RMSE) between models existing in the literature and the measurements.

Table 1. *Error estimators (MAE and RMSE) between data and existing models.*

	I_u (van den Hurk and Bruin (1995)		I_v (van den Hurk and Bruin (1995)		I_u (Luhar 2010)		I_v (Luhar 2010)	
	MAE	**RMSE**	**MAE**	**RMSE**	**MAE**	**RMSE**	**MAE**	**RMSE**
Jan	0.0587	0.0728	0.0650	0.0833	0.1493	0.1902	0.0609	0.0695
Feb	0.0561	0.0778	0.0562	0.0742	0.0708	0.088	0.1639	0.1924
Mar	0.0561	0.0748	0.0427	0.0560	0.0912	0.1099	0.1665	0.1914
Apr	0.0544	0.0658	0.0441	0.0575	0.0599	0.0722	0.1114	0.1374
May	0.0822	0.1209	0.0676	0.1025	0.1040	0.1371	0.1510	0.2088
Jun	0.099	0.1322	0.060	0.0822	0.0816	0.1052	0.1364	0.1825
Jul	0.0264	0.0365	0.0203	0.0265	0.0616	0.0781	0.1388	0.1852
Aug	0.0220	0.0263	0.0268	0.0349	0.0459	0.0576	0.1489	0.1984
Sep	0.0560	0.0721	0.0366	0.0453	0.0435	0.0549	0.1246	0.1620
Oct	0.088	0.1219	0.0611	0.0892	0.0785	0.1191	0.1567	0.2025
Nov	0.1208	0.1854	0.0968	0.1707	0.0765	0.1080	0.2484	0.3484
Dec	0.0813	0.1054	0.1039	0.1638	0.1197	0.1531	0.2570	0.3298

Analysis of Figure 13 and Table 1 reveal that the error estimators obtained with van den Hurk and the Bruin model are lower than the ones of Luhar, except the months of June, September, October, November for the longitudinal turbulence intensity and the months of January for the transversal turbulence intensity. The performance of these models is therefore better than that of Luhar's for most of the months. However, the inconsistencies pointed out by Luhar $\left(\sigma_u^2 = \sigma_v^2\right)$ could be the cause of the gap observed between the data and estimation during some months. In order to correct them and unlike the Luhar approach, we modified the existing formulation of [57] by introducing fitting parameters. Using Equations (9) and (11), the modified formulations of I_u and I_v are then expressed as follows:

$$I_u^2 = \frac{\left\{\kappa_k \sigma_U^2 - \lambda_b U^2 \left[\exp\left(-\frac{\zeta_n \sigma_\theta^2}{2}\right) - 1\right] + \mu_r\right\}}{2\tau_a U^2} \quad (17)$$

$$I_v^2 = \frac{\left\{A_n \sigma_U^2 - B_k U^2 \left[\exp\left(-C_r \sigma_\theta^2\right) - D_t\right]\right\}}{2E_j U^2} \quad (18)$$

From the algorithm fminsearch developed under Matlab, we determined the fitting coefficients, κ_k, λ_b, ζ_n, μ_r, τ_a, A_n, B_k, C_r, D_t, E_j of the modified formulations. The fminsearch function (based on the nonlinear least squares method) which allows finding the parameters that minimize the gap between the theoretical models and the experimental data from an initial estimate was used on Matlab R2013a (8.1.0.604) to determine these adjustment constants. The algorithm of this function uses the simplex search method of [74]. In Figure 15, we present the evaluation of the modified turbulence intensity formulations.

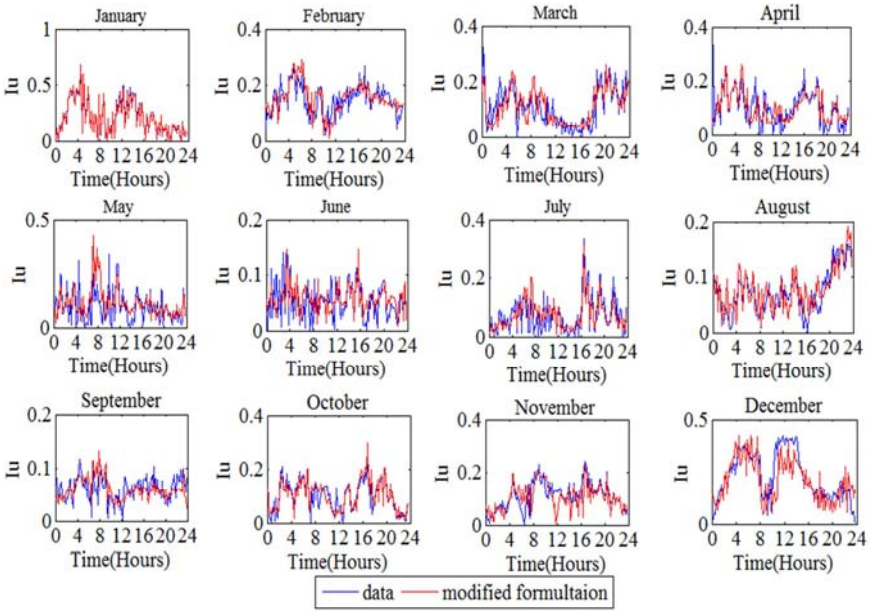

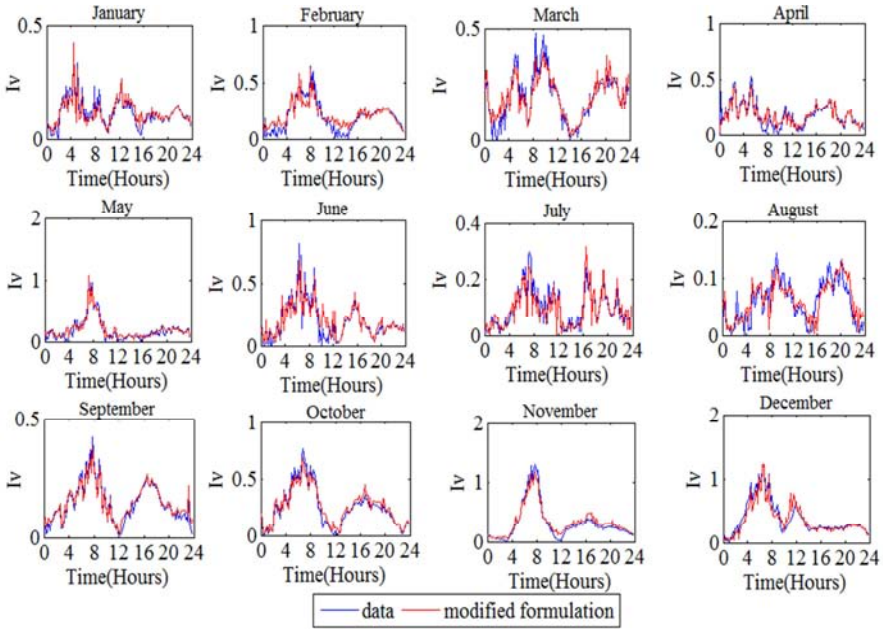

Figure 15. *Turbulence intensity fitting of the longitudinal and transversal wind components based on the new formulations (modified formulation) (2011-2014).*

In Tables 2 and 3 are presented the values of the fitting constants and the errors (MAE; RMSE) between the estimations obtained from the modified formulations and the measurements. Moreover, the estimation error reduction rate resulting from the modified formulations was evaluated.

Table 2. *Values of the adjustment constants and error estimators (MAE and RMSE) between modified formulations of longitudinal turbulence intensity and data.*

	Adjustment constant					I_u		**Error Reduction Rate (%)**
	κ_k	λ_b	ζ_n	μ_r	τ_a	**MAE**	**RMSE**	
Jan	-0.0141	-10	-0.35	-0.0007	1	0.0099	0.0141	83.13
Feb	-2.27	0.56	2	1.08	1	0.0291	0.0373	48.12
Mar	-0.0878	0.6229	2	0.07	1	0.0344	0.0447	38.68
Apr	-0.0379	0.5291	2	0.0676	1	0.0290	0.0418	46.69
May	-0.8477	3.3204	0.4009	0.2983	1	0.0450	0.0612	41.60
Jun	0.0011	-0.0156	0.0467	-0.0002	0.0982	0.0210	0.0267	74.26
Jul	0.9156	-0.0578	-17.9550	0.0036	1	0.0248	0.0316	6.06
Aug	4.6234	-0.5803	-3.0630	-0.1502	1	0.0183	0.0229	16.81
Sep	-0.9553	0.8631	0.5973	0.0797	1	0.0152	0.0192	65.05
Oct	0.0055	-0.0629	0.1090	-0.0002	1.2317	0.0177	0.0241	77.45
Nov	-0.0022	0.0055	0.1987	0.0001	0.25	0.0278	0.0405	63.66
Dec	-0.0001	0.0878	0.0008	0	0.0090	0.0577	0.0801	29.02

Table 3. *Values of the adjustment constants and error estimators (MAE and RMSE) between modified formulations of the transversal turbulence intensity and data.*

	Adjustment constant					I_v		**Error Reduction Rate (%)**
	A_n	B_k	C_r	D_t	E_j	**MAE**	**RMSE**	
Jan	0.4730	-0.0053	-5.796	1	0.25	0.0170	0.0245	72.08
Feb	0.4850	0.0355	-5.658	1	0.25	0.0419	0.0548	25.44
Mar	0.0079	0.1463	0.0280	1	0.0033	0.0270	0.0385	36.76
Apr	0.0033	0.0950	0.0290	1	0.002	0.0278	0.0449	36.96
May	0.6278	-0.0292	-4.1921	1	0.25	0.0398	0.0591	41.12
Jun	10^{-4}	0.1932	0.0006	1	$6.24\ 10^{-5}$	0.0328	0.0531	45.33
Jul	0.0003	0.0531	0.0203	1	0.00086	0.0180	0.0228	11.33
Aug	-0.2541	1.7296	0.1841	1	0.25	0.0151	0.0194	43.65
Sep	0.0005	0.0213	0.0243	1	0.00029	0.0136	0.0190	62.84
Oct	0.0004	0.0785	0.0048	1	0.00021	0.0328	0.0416	46.31
Nov	0.0003	0.3151	0.0012	1	0.00017	0.0519	0.0631	46.38
Dec	3.975	0.443	-1.648	1.061	1	0.0614	0.0890	40.90

Analysis of Figure 14 and Tables 2 and 3 show that the proposed modified formulations better reflect the distribution of the wind turbulence intensity (I_u and I_v) at our study site whatever the period of the day and year. Low values of the error estimators (MAE; RMSE) were recorded and vary from (0.0099; 0.0141) in January to (0.0577; 0.0801) in December for the longitudinal turbulence intensity and from (0.0136; 0.0190) in September to (0.0614; 0.0890) in December for the transversal turbulence intensity. The estimation error reduction rates obtained from these modified formulations vary between 6.06% and 83.13%. These two modified models therefore constitute reliable inputs for the evaluation of the loads induced by wind fluctuations on wind turbine blades.

4. Conclusions

The wind characteristics at 10 m above ground level along the Cotonou coast (Benin) that are essential to know before the installation of a wind turbine at a site have been studied and new estimators for the turbulence intensity of wind components have been proposed. The following concluding remarks can be made:

1. The highest monthly average speed are obtained in July and evaluated at (5.92 ± 0.17) $m.s^{-1}$, and the lowest one are recorded in November and estimated at (2.41± 0.55) $m.s^{-1}$. The most frequent winds come from southwest (SW) and south-southwest (SSW) directions whatever the season.
2. The annual average roughness length is evaluated at 1.25×10^{-4} m and the annual average friction velocity at 0.41 $m.s^{-1}$.
3. The turbulence intensity observed indicates high values in February, March, May, June, October, November, and December with peaks ranging from 0.2 to 0.6. On the other hand, during January, April, July, August and September, the values are low, especially in August where they do not exceed 0.12. These months are more suitable for an efficient exploitation of the wind resource available at the site.
4. The turbulence intensity observed at our site is an increasing linear function of the surface roughness. Pearson's correlation coefficient of the linear adjustment varies from 0.75 in January to 0.94 in August.
5. Finally, modified formulations of the longitudinal and transversal wind turbulence intensity obtained from the van den Hurk and de Bruin model and based on a best-fitting approach are proposed. The error estimators (MAE; RMSE) obtained to validate these modified models vary respectively from (0.0099; 0.0141) in January to (0.0614; 0.0890) in December respectively.

For optimal exploitation of wind energy at our study site, we suggest that the fatigue loads induced by the high turbulence levels observed at the site during the design of wind turbine blades should be taken into account. In the future, the turbulence integral length scale and the turbulence power spectra will be examined based on high-frequency wind data.

Acknowledgements

The authors of this paper sincerely thank the 'Institut de Recherche Halieutique et Océanographique du Bénin' (IRHOB) (the Beninese Institute for Fishery and Oceanographic Research) and the MCA (Millennium Challenge Account) Compact I for having made available to them the wind data used to carry out this work.

References

[1] A. M. M. Ismaiel, and S. Yoshida, "Study of turbulence intensity effect on the fatigue lifetime of wind turbines", Journal of Novel Carbon Resource Sciences & Green Asia Strategy, 2018, vol. 05, n° 1, pp. 25-32.

[2] Wind Power Monthly (2017), https://www.windpowermonthly.com/10-biggest-turbines.

[3] Global Wind Energy Council (2017), http://gwec.net/wp content/uploads/2018/02/Global_Cumulative_Installed_Wind _Capacity_2001-2017. jpg

[4] Z. L. Mahri, S. Zid, and R. M. Salah, "An optimal design of the wind turbine blade geometry adapted to a specific site using Algerian wind data", ROMAI J., 2013, vol. 9, n° 2, pp. 143-154.

[5] R. Rafiee, M. Moradi, and M. Khanpour, "The influence of material properties on the aeroelastic behavior of a composite wind turbine blade", Journal of Renewable and Sustainable Energy, 2016, vol. 8, pp. 1-12.

[6] I. Boumrar, "Effets de l'angle de calage des pales d'une petite éolienne sur sa puissance électrique générée". Third International Conference on Energy, Materials, Applied Energetics and Pollution ICEMAEP, 2016, Constantine, Algeria.

[7] Y. Kawashima, and T. Uchida, (2017), "Effects of terrain induced turbulence on wind turbine blade fatigue loads", *Energy and Power Engineering,* 2017, vol. 9, pp. 843-857.

[8] L. J. L. Stival, A. K. Guetter, and F. O. de Andrade, "The impact of wind shear and turbulence intensity on wind turbine power performance", Espaço Energia, 2017, 27, pp. 11-20.

[9] K. S. Hansen, R. J. Barthelmie, L. E. Jensen, A. Sommer, "The impact of turbulence intensity and atmospheric stability on power deficits due to wind turbine wakes at Horns. Rev wind farm", Wind Energy, vol. 15, n°1, pp. 183-196.

[10] L. C. Cheung, S. Premasuthan, S. Davoust, and D. von Terzi, A Simple Model for the Turbulence Intensity Distribution in Atmospheric Boundary Layers Journal of Physics: Conference Series, 2016, vol. 753, n°3, pp. 1-10.

[11] M. S. Siddiqui, A. Rasheed, T. Kvamsdal, and M. Tabib, "Effect of Turbulence Intensity on the Performance of an Offshore Vertical Axis Wind Turbine", Energy Procedia, 2015, vol. 80, pp. 312-320.

[12] S. T. Frandsen, "Turbulence and turbulence generated fatigue in wind turbine clusters, Report R–1188, Risø National Laboratory, Roskilde, 2007, Denmark.

[13] C. M. S. Martin, J. K. Lundquist, A. Clifton, G. S. Poulos, and S. J. Schreck (2016), ‘‘Wind turbine power production and annual energy production depend on atmospheric stability and turbulence’’, Wind Energ. Sci., 2016, vol. 1, pp. 221-236.

[14] R. J. Barthelmie, S. T. Frandsen, M. N. Nielsen, S. C. Pryor, P. E. Rethore, and H. E. Jørgensen (2007), ‘‘Modelling and measurements of power losses and turbulence intensity in wind turbine wakes at Middelgrunden offshore wind farm’’, Wind Energy, 2007, vol. 10, pp. 517-528.

[15] P. Adaramola, Å. Krogstad, ‘‘Experimental investigation of wake effects on wind turbine Performance’’, Renewable Energy, 2011, vol. 36, pp. 2078-2086.

[16] W. D. Lubitz, ‘‘Impact of ambient turbulence on performance of a small wind turbine’’, Wind Energy Applications (WE) World Renewable Energy Congress, Linköping, Sweden, 2011, pp. 4121-4127.

[17] T. Uchida, and Y. Ohya, ‘‘Latest Developments in Numerical Wind Synopsis Prediction Using the RIAM-COMPACTCFD Model Design Wind Speed Evaluation and Wind Risk (Terrain Induced Turbulence) Diagnostics in Japan’’, Energies, 2011, vol. 4, pp. 458-474.

[18] A. Sathe, J. Mann, T. K. Barlas, W. A. A. M. Bierbooms, and G. J. W. van Bussel, ‘‘Atmospheric stability and its influence on wind turbine loads. In Proceedings of Torque, the science of making torque from wind, 2012.

[19] A. Al-Abadi, Y. J. Kim, Ö. Ertunç, and A. Delgado, ‘‘Turbulence impact on wind turbines: experimental investigations on a wind turbine model’’, Journal of Physics: Conference Series, 2016, vol. 753, n°3, pp. 1-13.

[20] T. Uchida, ‘‘CFD Prediction of the Air flow at a Large scale Wind Farm above a Steep, Three- dimensional Escarpment’’, Energy and Power Engineering, 2017, vol 9, pp. 829-842.

[21] A. J. Eggers, R. Digumarthi, and K. Chaney, ‘‘Wind shear and turbulence effects on rotor fatigue and loads control’’ J. Sol. Energy Eng., 2003, vol. 125, pp. 402-409.

[22] T. Mücke, D. Kleinhans, and J. Peinke, ‘‘Atmospheric turbulence and its influence on the alternating loads on wind turbines’’, Wind Energy, 2000, vol. 14, n°2, pp. 301-316.

[23] A. J. Brand, J. Peinke, and J. Mann, ‘‘Turbulence and Wind Turbines, ECN Wind Energy, Wind turbine rotor and Wind farm Aerodynamics’’, 13th European Turbulence Conference Warsaw, Poland, 2011.

[24] T. Ishihara, A. Yamaguchi, and M. W. Sarwar, ‘‘A Study of the normal turbulence model in IEC 61400-1’’, Wind Engineering, 2012, vol. 36, n°6, pp. 759-766.

[25] A. Peña, R. Floors, A. Sathe, S. E. Gryning, R. Wagner, M. S. Courtney, G. Xiaoli, L. A. N. Hahmann, B. Charlotte, Y. Guo, J. Keller and W. La Cava, ‘‘Planetary gear load sharing of wind turbine drive trains subjected to non-torque loads’’, Wind Energy, 2015, vol. 18, n°4, pp. 757-768.

[26] H. Wang, R. J. Barthelmie, S. C. Pryor, and H. G. Kim, ‘‘A new turbulence model for offshore wind turbine standards’’, Wind Energ., 2013, vol. 17, pp. 1587-1604.

[27] A. K. Luhar (2010), ‘‘Estimating variances of horizontal wind fluctuations in stable condi- tions’’, Boundary-Layer Meteorol., 2010, vol. 135, pp. 301-311.

[28] T. S. Leu, J. M. Yo, Y. T. Tsai, J. J. Miau, and T. C. Wang (2014), ‘‘Assessment of IEC 61400-1 normal turbulence model for wind conditions in Taiwan West Coast areas’’, 5th International Symposium on Physics of Fluids (ISPF5), International Journal of Modern Physics: Conference Series, 2014, vol. 34, pp. 1-8.

[29] N. Cheggaga, A. Hamidat, O. Nadjemi, ‘‘Génération de profils de vent en vue d’application éoliennes’’, IJEST, 2015, vol. 3, pp. 97-102.

[30] F. Porté-Agel, Y. T. Wu, C. H. Chen, ‘‘A Numerical study of the effects of wind direction on turbine wakes and power losses in a large wind farm’’, Energies, 2013, vol. 6, pp. 5297-5313.

[31] S. Madougou, ‘’Etude du potentiel éolien du jet nocturne dans la zone sahélienne à partir des observations de radars profilers de vent’’, Thèse de Doctorat, Université Paul Sabatier III, Toulouse, France, 2010.

[32] M. Nadjah, M. Khechana, L. Laiche, T. Ouksel, and C. Mahfoudi, ‘‘Etude de l’hélice d’une éolienne de 5 kW’’, Revue des Energies Renouvelables, 2008, pp. 257-264.

[33] B. Attaf, ‘‘Eco-conception et développement des pales d’éoliennes en matériaux composites’’, Revue des Energies Renouvelables, 2010, pp. 37-48.

[34] C. N. Awanou, J. M. Degbey, and E. Ahlonsou, ‘‘Estimation of the mean wind energy avaible in Benin (ex Dahomey)’’, Renew. Energy, 1991, vol. 1, n°40, pp. 845-853.

[35] M. A. Houekpoheha, B. Kounouhewa, B. N. Tokpohozin, and C. N. Awanou, ‘‘Estimation de la puissance énergétique éolienne à partir de la distribution de weibull sur la côte béninoise de Cotonou dans le golfe de guinée’’, Revue des Energies Renouvelables, vol. 17, 2014, pp. 489-495.

[36] A. B. Akpo, J. C. T. Damada, H. E. V. Donnou, B. Kounouhewa, B. and C. N. Awanou (2015), ‘‘Estimation de la production énergétique d’un aérogénérateur sur un site isolé dans la région côtière du Bénin’’, Revue des Energies Renouvelables, 2015, vol. 18, n°3, pp. 457-468.

[37] B. E. Houngninou, C. S. U. Allé, K. F. Guédjé, H. Kougbéagbédè, ‘‘Changes in near-surface wind speed in the south of Benin from 1961 to 2016’’, Int. J. Adv. Res., 2017, vol. 5, n°11, pp. 1223-1232.

[38] E. Richard, and A. Dolle, ‘‘Data Report (MCA): Development of a metocean station at the port of cotonou: Supply, installation, operation and maintenance of an oceanographic monitoring: (lot5)’’, pp8- atm - 145c, Millennium Challenge Account (MCA I Benin). 2011.

[39] C. Thomas, and T. Foken, ‘‘Re-evaluation of integral turbulence characteristics and their parameterisations’’, Am. Meteorol. Soc, 2002, pp. 129-132.

[40] Z. Sorbjan, An examination of local similarity theory in the stably stratified boundary layer’’, Boundary-Layer Meteorol, 1987, vol. 38, pp. 63-71.

[41] Q. Zhang, J. Zeng, T. Yao (2012), ‘‘Interaction of aerodynamic roughness length and wind-flow conditions and its parameterization over vegetation surface’’, Atmospheric Science, 2012, vol. 57, n°13, pp. 1559-1567.

[42] A. S. Monin, A. M. Obukhov, ‘‘Basic Laws of Turbulent Mixing in the Ground Layer of the Atmosphere’’, Akad. Nauk SSSR Geofiz. InstTr, 1954, vol. 151, pp. 163-187.

[43] C. A. Paulson, ‘‘The mathematical representation of wind speed and temperature profiles in the unstable atmospheric surface layer. J. Appl. Meteorol, 1970, vol. 9, pp. 857-861.

[44] J. A. Businger, J. C. Wyngaard, Y. Izumi and E. F. Bradley, ‘‘Flux-Profile relationships in the atmospheric surface layer’’, J. Atmos Sci., 1971, vol. 28, n°18, pp. 181-189.

[45] R. O. Weber, ‘‘Estimators for the standard deviations of lateral, longitudinal and vertical wind components’’, Atmos. Environ., 1998, vol. 32, pp. 3639-3646.

[46] J. Bengtsson, ‘‘Turbulence wind flow modeling in complex Terrain: A comparison between a linear model, a CFD model and a NWP Model’’, Master’s thesis, Chalmers University of Technology Göteborg, Göteborg, Sweden. 2015.

[47] A. Mostafaeipour, M. Jadidi, K. Mohammadi, and A. Sedaghat, ‘‘An Analysis of Wind Energy Potential and Economic Evaluation in Zahedan, Iran’’, Renewable and Sustainable Energy Reviews, 2014, vol. 30, pp. 641–650.

[48] H. Charnock, ‘‘Wind stress on a water surface’’, Quarterly Journal of the Royal Meteorological Society, 1955, vol. 81, pp. 639-640.

[49] A. Peña, and S. E. Gryning, ‘‘Charnock’s roughness length Model and non-dimensional wind profiles over the sea’’, Boundary-Layer Meteorol., 2008a, vol. 128, pp. 191-203.

[50] A. Obermann, B. Edelmann and B. Ahrens, ‘‘Influence of sea surface roughness length parameterization on Mistral and Tramontane simulations’’, Adv. Sci. Res., 2016, vol. 13, pp. 107-112.

[51] M. A. Donelan, F. W. Dobson, S. D. Smith, and R. J. Anderson, ‘‘On the dependence of sea surface roughness on wave development. Journal of Physical Oceanography, 1993, vol. 23, pp. 2143-2149.

[52] R. J. Barthelmie, ‘‘Evaluating the impact of wind induced roughness change and tidal range on extrapolation of offshore vertical wind speed profiles’’, Wind Energ, 2001, vol. 4, pp. 99-105.

[53] M. Turk, and S. Emeis, ‘‘The dependence of offshore turbulence intensity on wind speed. J. Wind Eng. Ind. Aerodyn, 2010, vol. 98, pp. 466-471.

[54] M. Mirhosseini, F. Sharifi, and A. Sedaghat, ‘‘Assessing the wind energy potential locations in province of Semnan in Iran, Renew Sustain Energy Rev, 2011, vol. 15, pp. 449-59.

[55] J. F. Manwell, J. G. McGowan, A. L. and Rogers (2009), Wind energy explained: theory, design and application, 2nd ed, Chichester, U. K., Wiley.

[56] X. Zidong, W. Hao, W. Teng, T. Tianyou, and M. Jianxiao, ‘‘Wind characteristics at Sutong Bridge site using 8-year field measurement data’’, Wind Struct, 2017, vol. 25, n°2, 195-214.

[57] B. J. J. M van den Hurk, and H. A. R. de Bruin, ‘‘Fluctuations of the horizontal wind under unstable conditions’’, Boundary-Layer Meteorol., 1995, vol. 74, pp. 341-352.

[58] M. C. Cirillo, and A. A. Poli, ‘‘An intercomparison of semi empirical diffusion models under low wind speed, stable conditions, Atmos Environ.., 1992, vol. 26, pp. 765-774.

[59] F. Ben Amar, M. Elamouri, and M. R. Dhifaoui, ‘‘Energy Assessment of the First Wind Farm Section of Sidi Daoud, Tunisia’’, Renew. Energy, 2008, vol. 33, n°10, pp. 2311-2321.

[60] T. Chai, R. R. Draxler, ‘‘Root mean square error (rmse) or mean absolute error (mae) ?- arguments against avoiding rmse in the literature’’, Geosci. Model Dev., 2014, vol. 7, pp. 1247–1250.

[61] D. Petkovic, S. Shamshirband, N. B. Anuar, H. Saboohi, A. W. Abdul Wahab, M. Protic, E. Zalnezhad, and S. M. Amin Mirhashemi, ‘‘An appraisal of wind speed distribution prediction by soft computing methodologies: A comparative study’’, Energy Conversion and Management, 2014, vol. 84, pp. 133-139.

[62] S. M. Ogbonmwan, E. T. Ogbomida, N. O. Uwadia, O. R. Efegoma, and G. L. Umoru, ‘‘Analysis of trends in the variability of monthly mean minimum and maximum temperature and relative humidity in Benin City’’, Int. J. Renew. Energ & Environ., 2016, vol. 2, pp. 150-165.

[63] A. S. Bajamgnigni Gbambie, and D. G. Steyn, ‘‘Sea breezes at Cotonou and their interaction with the West African monsoon’’, Int. J. Climatol, 2013, vol 33, pp. 2889-2899.

[64] D. Khalfa, A. Benretem, L. Herous, and I. Meghlaoui, ‘‘Evaluation of the adequacy of the wind speed extrapolation laws for two different roughness meteorological sites’’, Am. J. Appl. Sci., 2014, vol. 11, n°4, pp. 570-583.

[65] A. Peña, S. E. Gryning, and C. B. Hasager, (2008b), ‘‘Measurements and modelling of the wind speed profile in the marine atmospheric boundary Layer’’, Boundary-Layer Meteorol., 2008b, vol. 129, pp. 479-495.

[66] D. Jarmalavičius, J. Satkūnas, G. Zilinskas, and D. Pupienis, ’’ The influence of coastal morphology on wind dynamics, ’’ Estonian Journal of Earth Sciences, 2012, vol. 61, n°2, pp. 120-130.

[67] T. Meada, T. Yokota, Y. Shimizu, and K. Adachi, ‘‘Wind tunnel study of the interaction between two horizontal axis wind turbines’’, Wind Eng, 2004, vol. 8, n°2, 197-212.

[68] S. Chowdhury, J. Zhang, A. Messac, and L. Castillo, ‘‘Optimizing the arrangement and the selection of turbines for wind farms subject to varying wind conditions’’, Renewable Energy, 2013, vol. 52, pp. 273-282.

[69] T. R. Ayodele, and A. S. O. Ogunjuyigbe, ‘‘Assessment of turbulence intensity of local wind regimes’’, International Journal of Sustainable Energy, 2014, vol. 35, n°3, pp. 1-14.

[70] R. L. Petersen, ‘‘A wind tunnel evaluation of methods for estimating surface roughness length at industrial facilities’’, Atmospheric Environment, 1997, vol. 31, n°1, pp. 45-57.

[71] H. W. Tieleman, ‘‘Roughness estimation for wind-load simulation experiments’’, J. Wind. Eng. Ind. Aerodyn, 2003, vol. 91, pp. 1163-73.

[72] M. C. H. Hui, A. Larsen, and H. F. Xiang, ‘‘Wind turbulence characteristics study at the Stonecutters Bridge site: Part I-Mean wind and turbulence intensities. J. Wind Eng. Ind. Aerodyn, 2009, vol. 97, pp. 22-36.

[73] G. Gualtieri, and G. Zappitelli, G. (2015), ‘‘Investigating wind resource, turbulence intensity and gust factor on mountain locations in Southern Italy’’, Int. J. of Green Energy, 2015, vol. 12, n°5, pp. 309-327.

[74] J. C. Lagarias., J. A. Reeds, M. H. Wright, and P. E. Wright, (1998), ‘‘Convergence Properties of the Nelder-Mead Simplex Method in Low Dimensions’’, SIAM Journal of Optimization, 1998, vol. 9, n°1, pp. 112-147.